Thrust Measuring System for Electrothermal Thrusters

B. C. BARBER*
Royal Aircraft Establishment, Farnborough, Hampshire, England

A fast response thrust and impulse measuring system is described. The system has a risetime of 2.5 *m*sec, measures thrust in the range 2 mN–200 mN with 5% accuracy and worst case signal to noise ratio of 20 db. It is suitable for use with small electrothermal thrusters. The thruster is attached to a single-degree-of-freedom mass spring system, lightly damped, and with a period of about 30 msec. The displacement of this combination is proportional to the thrust modified by the transfer function of the mass-spring system. A signal proportional to the displacement is processed by an electronic circuit having the inverse transfer function, and the resulting output gives the thrust. The impulse is then directly obtained by electronically integrating the thrust function.

Introduction

RECENTLY proposed attitude control systems employ electrothermal thrusters in a wheel damping mode.[1] These thrusters operate for times of the order of hundreds of milliseconds at thrust levels of 100–200 mN. They are also usually designed to operate at greatly reduced impulse bits with pulse-widths of tens of milliseconds to maintain attitude control in the event of the wheel system failing, thus providing a backup system. The fastest electrothermal thrusters appear to have plenum pressure risetimes of the order of 10 *m*sec and fall times of 20 *m*sec.[2] Thrust rise/fall times would be expected to be of the same order. At low plenum pressures the nozzle efficiency is usually low and thus, during the rise and fall periods, the specific impulse is low. Therefore for pulse widths of tens of milliseconds, the thruster is operating at a low specific impulse over a significant proportion of the pulse. Hence it is necessary to reduce the rise and fall times as far as possible to maintain a reasonable specific impulse at low impulse levels. The thrust rise and fall times are therefore important parameters and should be measured.

Thrust information may be obtained from plenum pressure measurements. However this method relies on accurate knowledge of the nozzle characteristics, both for steady-state and for transient flow. Furthermore assumptions must be made regarding the composition and thermodynamic properties of the exhaust. The most reliable approach is to measure the thrust directly with a fast response thrust transducer and this is the approach adopted here. This solution has other attractions. By integrating the thrust over the pulse width the impulse may be evaluated directly, and the impulse produced by a train of pulses may be evaluated, as may the impulse produced by any individual pulse in a pulse train. Other impulse measuring techniques, e.g., a ballistic pendulum, do not have this flexibility. Furthermore certain types of thruster (principally those operating with hydrazine propellant) can develop "roughness" and it is desirable to be able to measure these thrust oscillations.

A system risetime of 2.5 msec corresponds to a bandwidth (to -3 db) of about 180 Hz and would cause an error of about 3% in the measurement of a 10 *m*sec risetime, assuming that risetimes add vectorially. The pressure oscillations present in these thrusters appear to cover a band from 50 Hz to 150 Hz; 2.5 *m*sec is therefore about the optimum system risetime.

Presented as Paper 73-1065 at the AIAA 10th Electric Propulsion Conference, Lake Tahoe, Nev., October 31–November 2, 1973; submitted November 9, 1973; revision received April 3, 1974.

Index categories: Spacecraft Attitude Dynamics and Control; Rocket Engine Testing; Research Facilities and Instrumentation.

* Scientific Officer, Space Department.

Thrust and Impulse Measuring Techniques

Thrust measuring transducers must essentially be mass-spring systems with the thruster forming part of the mass. The "spring" force may be restoring force provided by gravity, by a mechanical spring, or by an electromechanical actuator in the case of a force-feedback system. To achieve a given bandwidth for time-resolved measurements, the system must either have a fundamental resonant frequency far above the required frequency band with associated damping and/or filtering, or a fundamental within the frequency band with the displacement signal processed by a transformation technique. Systems which have a high resonant frequency can work well when the thruster has a relatively high thrust and low mass. Recent thrusters, however, often have masses of several hundred grams. In such cases to achieve the required resonant frequency (several hundred hertz for a 2.5 *m*sec risetime) the transducer has to be so stiff that the displacement is less than 10^{-8} microinch at the operating thrust levels. It is very difficult to measure such a small displacement reliably because of temperature fluctuations and creep. Such a transducer using a piezoelectric element to measure displacement and provide the (spring) restoring force has been constructed at RAE. It has been found to have dc stability problems. The frame of the transducer distorts and creeps very slightly and causes considerable drift. The most sensitive charge amplifier/piezoelectric transducer combination available has to be operated beyond its capabilities with the result that charge amplifier drift can easily exceed the measured thrust. In addition there is the usual charge leakage associated with all piezoelectric transducers. Force-feedback systems have other problems. Experience has shown that mechanical resonances present in the thruster are excited by the actuator providing the feedback force. In fact these mechanical resonances appear as LCR networks within the feedback loop and cause severe stability problems. The resonances may be mitigated by including networks with suitable transfer functions within the feedback loop, but these networks invariably become very complex and difficult to formulate. Moreover, each thruster must be treated individually.

Inverse transform techniques allow the transducers to have a low resonance (within the frequency band of interest) and in consequence, a much greater sensitivity. The stiffness of a mass spring system is proportional to the square of the natural frequency, so that reducing the fundamental from, say, 200 Hz to 20 Hz increases the sensitivity by a factor of 100. Because displacements are of a reasonable magnitude (of the order of a micron in the case of the RAE thrust transducer), temperature fluctuations and creep difficulties become insignificant. In fact, with the present transducer, there have been no problems with dc stability. Moreover, such a technique is of an open-loop character and there are no feedback stability problems.

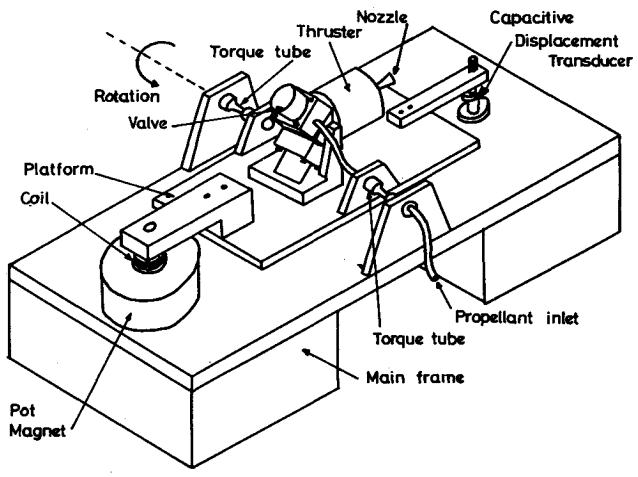

Fig. 1 Fast response thrust transducer.

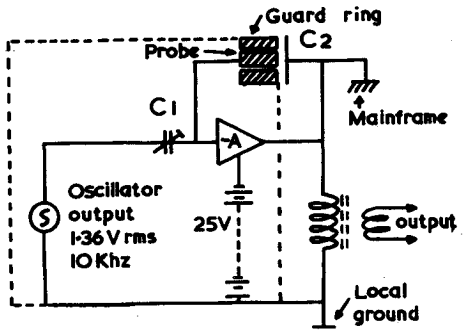

Fig. 2 Displacement transducer schematic.

Inverse Transform Technique

If the torque presented to the transducer by the thruster is $T(t)$, the spring torque constant is k, the damping factor is c, and the moment of inertia I, the equation of motion for a torsional mass-spring system (i.e., the thrust transducer) is

$$I\ddot{\theta}+c\dot{\theta}+k\theta = T(t)$$

The angular displacement θ may be measured by a displacement transducer. This signal is operated on using operational amplifier techniques to give the three terms $I\ddot{\theta}$, $c\dot{\theta}$, and $k\theta$. These terms are then summed to give $T(t)$, which apart from a numerical constant, is the required thrust function. $T(t)$ is finally filtered to remove noise and define the system bandwidth. From the standpoint of operational calculus one is, of course, setting up the inverse of the transfer function of the mechanical system.[3] Hence the term "inverse transform."

If the mechanical system has little damping it is possible to ignore the velocity term $(c\dot{\theta})$. The acceleration term $I\ddot{\theta}$ may then be derived from an accelerometer attached to the thruster. This technique is known as "accelerometer compensation" and has been employed on rocket motor thrust stands measuring thrusts of the order of 250 N[4] and 5000 N.[5-7]

The thruster force, as derived from the inverse transform, is usually distorted by small oscillations derived from the mechanical resonances present in the thruster. This is a result of approximating an essentially multidegree of freedom system by a single degree of freedom. It is possible to remove these distortions by introducing further inverse transforms,[3] or by filtering. To avoid introducing any overshoot or ringing into the electronic circuitry, the filter must be of a type having a linear phase characteristic. Such filters unfortunately have a very slow amplitude cutoff[8] and unnecessarily limit the bandwidth. The cutoff may be made more rapid without unduly distorting the phase response by introducing zeros into the stopband.[9] This has the advantage that if a particular resonance is troublesome it may be removed by introducing a zero at that frequency. This is only possible, of course, if the resonance lies above the passband. It has been found that this is often the case and so recourse to further inverse transforms has usually proved unnecessary.

Thrust Transducer

The thrust measuring transducer is shown in Fig. 1. The thruster is rigidly mounted on an aluminum alloy platform measuring 160 mm long, 180 mm wide, and 6 mm deep. The platform is mounted on to the mainframe of the transducer by two torque tubes. Each torque tube has a length of 35 mm and an inside diameter of 2.5 mm with a wall thickness of 0.25 mm over a length of 5 mm. They are made from 14% tungsten-vanadium tool steel and fully heat treated. These tubes provide the spring restoring force. One tube carries the propellant and the other carries electrical wires. This arrangement ensures that the propellant flows along the axis of rotation. There can thus be no spurious effects caused by the propellant pressure and viscosity and both liquid and gaseous propellants can be accommodated. Moreover, this arrangement has a very high lateral rigidity and helps to ensure that the transducer has only a single degree of freedom. In this connection it is essential to ensure that the clamps holding the torque tubes to the platform and to the mainframe are very rigid and that the tubes are mounted on the same axis to avoid bending.

The thruster provides a torque which rotates the platform against the restoring force of the torque tubes. This rotation is measured by a capacitive transducer mounted on the mainframe and acting on an arm rigidly attached to one end of the platform. At the other end an arm carries a coil which moves inside a pot magnet attached to the mainframe. The space between the coil and the magnet pole pieces is filled with silicon vacuum oil which provides a small amount of damping. Silicon oil is an ideal choice since it retains an almost constant viscosity up to quite high temperatures—the platform can become quite hot if there is a large heat flux leakage from the hot thruster to its mounting.

The coil operates in the same way as a loudspeaker coil and is used to calibrate the transducer dynamically. Current pulses of known shape are fed through the coil and the inverse transform adjusted until the indicated force is the same as the input.

Very great care is needed in the design of the transducer to avoid mechanical resonances within the frequency band of interest. All fittings and fixtures have to be made very rigid. The platform in particular can have many resonances and the present dimensions were arrived at after considerable calculation and experimentation. In the present design the most serious resonance is a lateral oscillation of the whole platform up and down caused by the torque tubes bending and stretching very slightly. Fortunately this resonance occurs at from 600 Hz to 750 Hz depending on the mass of the thruster, and is well outside the 0 Hz to 200 Hz band. The thrust transducer is very sensitive to ground vibrations and in order to reduce these as far as possible the transducer mainframe is hung on eight coil springs. The transducer weighs some 40 kg wt and this weight in conjunction with the springs forms an effective low-pass mechanical filter. The

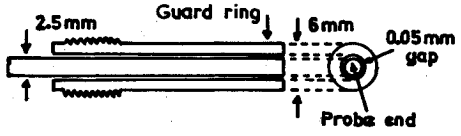

Fig. 3 Transducer probe. Capacitance at FSD = 0.35 $\mu\mu f$.

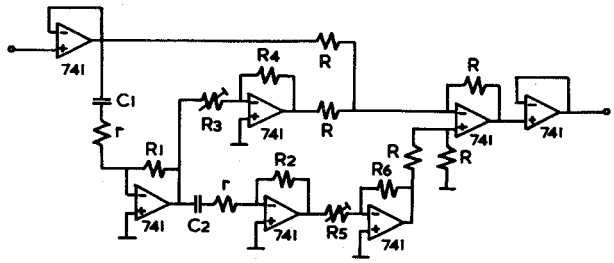

Fig. 4 **Inverse transform schematic.** $V_{out} = [1 + C_1R_1(R_4/R_3)(d/dt) + C_1R_1C_2R_2(R_6/R_5)(d^2/dt^2)]V_{in}$.

movement of the frame under the influence of a 100 mN thruster is completely undetectable.

Displacement Measuring Circuit

The inverse transform contains a double differentiator which is very sensitive to noise. It is therefore absolutely essential that the electrical noise present in the displacement measuring circuitry be kept as low as possible. Commercial displacement transducers were found to be too noisy so a transducer was specially developed. The schematic is shown in Fig. 2. The high gain amplifier has a gain of about 70 db at 10 kHz and the gain is tailored to fall off either side at 6 db/octave initially and finally at about 10 db/octave at 20 MHz where the gain becomes unity. At the low frequency end the gain becomes unity at about 3 Hz. This ensures loop stability. The capacitive transducer is connected in a feedback loop around the amplifier. A guardring around the center electrode of the probe ensures linearity.

The gain of this feedback configuration $= (-C_1/C_2)$; C_1 is constant (at about 0.5 pF) and C_2 is the feedback capacitance, in this case the capacitance between the probe and arm bolted to the platform. The capacitance of the probe and arm $= k/d$ where k is an arbitrary constant and d is the probe-arm separation. Hence if a constant ac signal is applied to C_1 the output voltage is directly proportional to d.

The oscillator and amplifier are contained within the mainframe of the unit and are powered by an integral 25 v rechargeable battery which can be recharged at will from an external control unit. During normal operation the battery, amplifier and oscillator are isolated from external circuitry except for the output which is transformer isolated. These elaborate precautions were found to be necessary to eliminate low frequency noise present in the mains power lines. The oscillator, amplifier, and battery are screened by the steel mainframe of the transducer. The displacement circuit has a full-scale output at a separation of 125 μm and has a measured linearity of 0.2% up to full scale deflection (FDS). The oscillator is designed to give a constant voltage output irrespective of supply voltage and temperature and holds its output to within 0.5% up to 110°C. A static load can therefore be measured to within 1% under any conceivable circumstance.

The displacement output is in the form of an amplitude modulated 10 kHz carrier. This is demodulated and filtered by an

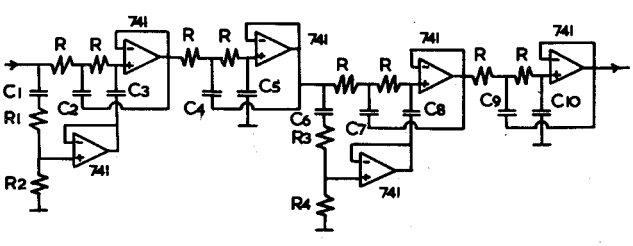

Fig. 5 **Storey and Cullyer linear phase filter schematic.**

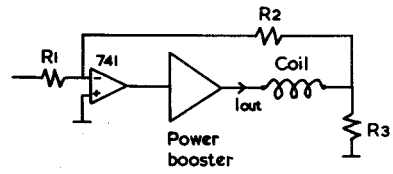

Fig. 6 **Calibrator schematic.** $I_{out} = V_{in}(R_2/R_1)(1/R_3)$.

eighth-order linear phase filter with a −3 db frequency of 1.5 kHz. The displacement signal is then fed to the inverse transform.

Inverse Transform

The schematic of the inverse transform is shown in Fig. 4. Differentiators and particularly double differentiators can be unstable since their gain increases with frequency. It is therefore necessary to modify the response of a practical differentiator by curtailing its gain at high frequency. This is done in this circuit by including the resistors r in series with the capacitors C_1 and C_2. The corner frequency of the differentiators is set at about 1 kHz, well outside the 200 Hz band edge of the following filters. Hence the circuit accurately reproduces the required transfer function within the pass band. The damping and inertia coefficients are set separately by R_3 and R_5. By arranging the gains of each differentiator to be set in this way it is possible to calibrate R_3 and R_5. The undamped natural frequency of the transducer is measured and set up on the R_3 dial and the R_5 dial set to kn^2 where k is a calibration constant and n the natural frequency. The damping oil is added and the transducer and inverse transform are ready for operation. It should be pointed out that Fig. 4 is not the only way of achieving the required transfer function.[3]

It has been found necessary to screen all parts of the transform and to buffer the input and output to ensure adequate stability. The output of the transform is filtered by one or two eighth order Story and Cullyer linear phase filters. The circuit of a typical filter is shown in Fig. 5. The filter is constructed using Sallen and Key sections instead of the negative impedance converters used by Storey and Cullyer.[10] It is usually necessary to employ two such filters giving a total of four zeros. High-frequency resonances can then be almost entirely eliminated.

Calibrator

The calibrator schematic is shown in Fig. 6. It consists of a standard voltage to current converter circuit. Pulses of from 10 $m$sec to 1 sec duration at preset amplitudes can be input to the converter that feeds corresponding current pulses through the coil attached to the platform. The coil movement is typically of the order of 1 μm and can thus be considered to move in a region of constant magnetic flux. Hence the force applied by the coil to the platform is directly proportional to the current and any force function can be applied. This enables the inverse transform to be set up and gives confidence in its correct functioning.

Calibration and Setting the Inverse Transform

The static sensitivity of the transducer is calibrated by means of weights attached to the transducer platform. Pulses are then fed to the calibrator with an amplitude sufficient to give a deflection corresponding to the deflection caused by the static weights. The damping factor of the transducer is low. It takes some twenty oscillations for the platform to stabilise and hence the contribution of the velocity channel is small. Initially therefore the velocity channel is switched off and the acceleration channel adjusted until the output force pulse approximates to the input current pulse. The velocity channel is then switched on and adjusted to remove the final distortions. A typical calibration pulse is shown

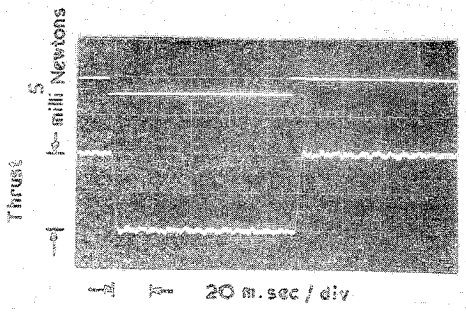

Fig. 7 Typical calibration pulse.

in Fig. 7. The upper trace is the current pulse through the coil and the lower trace is the filtered output of the inverse transform. The pulse duration is nominally 100 *m*sec, the risetime is 2.5 *m*sec and has an amplitude of 0.25 *m*/N/m. This represents the ultimate sensitivity of the present transducer and represents a thrust of 5 mN on a 50 mm torque arm. The signal-to-noise ratio is about 20 db and worsens rapidly at lower thrust levels. This noise is mainly ground vibration with the addition of high frequency resonances.

Operation of the Transducer with a Thruster

Most thrusters have a propellant flow control valve attached. This valve can produce considerable reaction forces. The pulses in Fig. 8 are reaction transients produced by a small flow control valve. The first two spikes correspond to the valve opening and the last two to the valve closing. The interval between the valve opening and closing is nominally 100 *m*sec and the peak amplitude of the spikes is about 70 mN. The first downward spike is caused by the valve armature accelerating away from the valve seat and producing a reaction force on the force transducer. This reaction reverses when the armature slows down at the end of its travel and this is the next upward spike. The situation is reversed when the valve closes except that the last downward spike has a double peak showing that the valve armature bounces off the valve seat.

These valve reaction forces distort the leading and trailing edges of the thrust pulse. Furthermore, the reaction spikes tend to excite resonances on the thruster and these distort the thrust pulse even more. Fig. 9 shows the thrust produced by a small thruster having a risetime of about 12 *m*sec and producing a thrust of about 60 mN with a nominal pulse width of 30 *m*sec. The system risetime in this case is 2.5 *m*sec. Figure 10 shows the same thrust pulse but with a system risetime of 5 *m*sec obtained by switching further filters. The valve reaction spikes are clearly visible as is the effect of reducing the bandwidth. Figure 10 shows a much cleaner trace than Fig. 9, but at the expense of slightly slowing up the observed rise and fall. The amplitude of the valve reaction spikes in Fig. 10 is also much reduced. Apart from the spikes, the trace shows the typical exponential rise-exponential fall pulse obtained from gasdynamic thrusters.

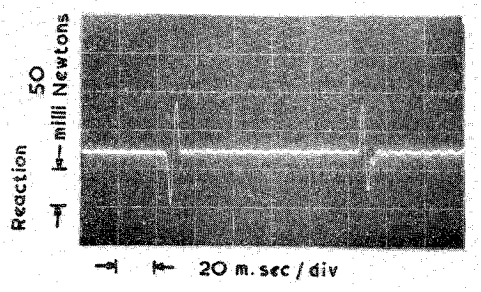

Fig. 8 Valve reaction transients.

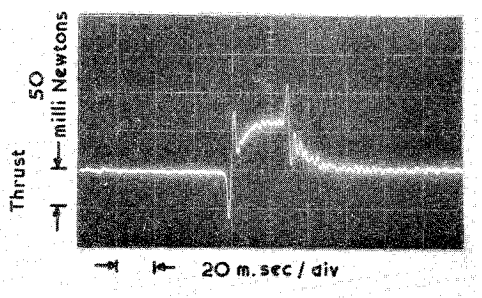

Fig. 9 30 msec thruster pulse: 2.5 msec system risetime.

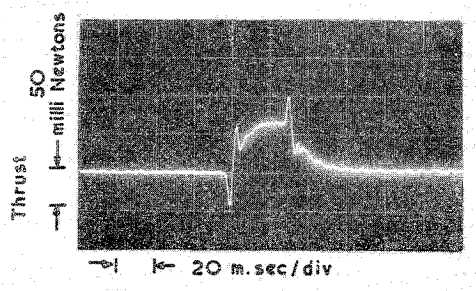

Fig. 10 30 msec thruster pulse: 5.0 msec system risetime.

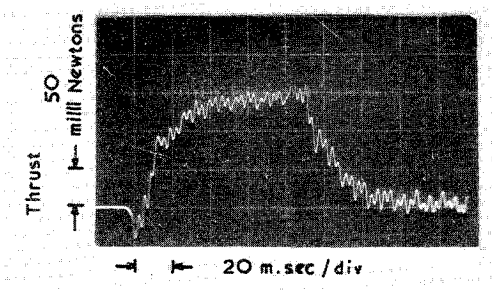

Fig. 11 Resisto-jet thrust pulse.

Figure 11 shows the thrust obtained from a small resisto-jet. This particular thruster has a large number of resonances and these distort the trace considerably. The thrust amplitude is 50 mN and the pulse width is 45 *m*sec. The time constant of the exponential rise and fall is about 10 *m*sec. The resonances are excited by the valve spikes which are visible but buried in the noise. It is possible to separate the valve from the thruster and mount the valve on to the mainframe of the transducer. This, however, increases the time constant of the thrust pulse since extra pipe volume is introduced between the thruster and valve.

Figure 12 shows the various components of the inverse transform signal corresponding to the thrust pulse in Fig. 10. The

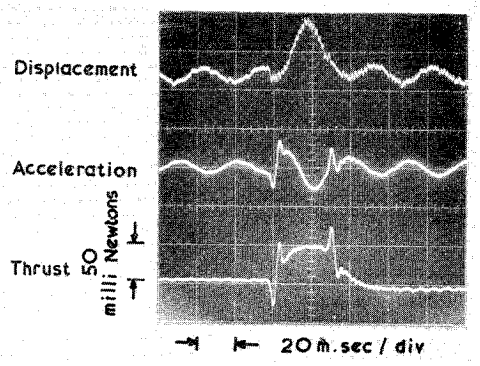

Fig. 12 Inverse transform components: no system damping.

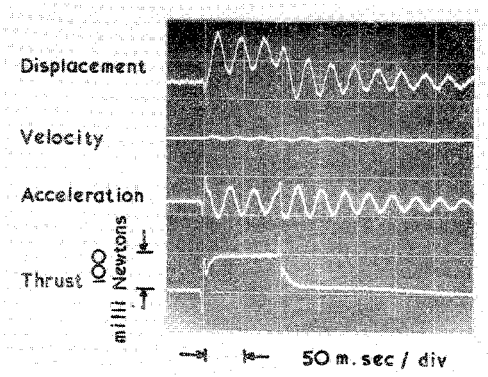

Fig. 13 Inverse transform components: with damping.

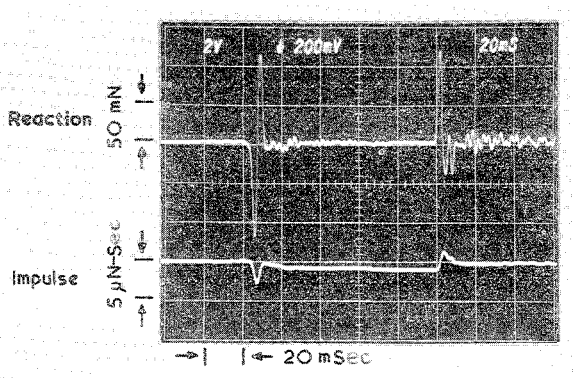

Fig. 15 Impulse produced by valve reaction transients.

top trace is the displacement of the platform. In this case the platform was completely undamped. The middle trace is the output of the acceleration channel and the bottom trace, traces 1 and 2 summed and filtered. In this case there was no damping and hence the velocity channel was not used. It is quite possible to use the system completely undamped, but repetition pulsing can cause problems if the natural frequency of the transducer approaches a harmonic of the thruster repetition frequency. It is usually best to provide for a small amount of damping and Fig. 13 shows the outputs from the various channels in such a case. The pulse has a width of 100 *m*sec and an amplitude of 100 mN. The thruster shows rise and fall times of about 15 *m*sec. The top trace is the displacement of the platform, the second trace the output of the velocity channel, the third trace the output of the acceleration channel and the bottom trace is the thrust pulse and is the sum of the top three traces. Note that the phase difference between the oscillations in the first and third traces is 180° and the phase difference between the displacement and velocity channels is 90°. It will be noted in Fig. 13 that the thrust does not settle back down to zero until about 250 *m*sec after the end of the pulse. It is thought that this "tail" is caused by gas within the thruster slowly leaking out of the nozzle after the main bulk of the propellant has been exhausted.

Impulse Measurement

The impulse corresponding to a particular thrust pulse is obtained simply by integrating the thrust pulse. Figure 14 shows a type of "track and hold integrator" which has been used to obtain the impulse data shown in Figs. 15–17. Figure 14 is a standard integrator except for the inclusion of C_1. Under quiescent conditions relay contacts 1*a* and 1*b* are closed. Thus the integrating capacitor C and capacitor C_1 charge to the standing dc potential at the integrator input (the output of the integrator remaining at zero). When the circuit is required to integrate contacts 1*a* and 1*b* open. The integrator then only integrates any *change* in input voltage. This eliminates any need to set the standing dc potential at the integrator input to zero. The amplifier must, of course, have a very low input current requirement (an fet input operational amplifier), otherwise C_1 would change its charge during the integration.

Figure 15 shows the impulse produced by the valve reaction spikes. The maximum impulse at any point is about 2.5 μN-sec and over one complete operation the impulse sums to zero, as it should. Figure 16 shows the impulse produced by a succession of 100 *m*sec pulses of about 110 mN amplitude. The total impulse produced by the six pulses is about 59 μN-sec. Figure 17 shows the impulse produced by just one of the same pulses. The indicated impulse is 10 *m*N-sec.

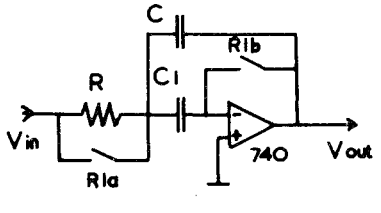

Fig. 14 Impulse integrator schematic.

$$(1/RC)\int_0^t \Delta V \, dt.$$

Conclusion

It has been demonstrated that techniques used for the dynamic thrust measurement of rocket motors can be applied successfully to small thrust stands measuring thrusts some five orders of magnitude smaller with adequate system risetimes. Problems exist with mechanical resonances present in these thrusters being excited by reaction spikes from the propellant control valve. However, these second-order distortions can (in principle) be removed by further inverse transforms.

Impulse data is readily obtained from the thrust transducer by integrating the output. Furthermore the impulse measurements

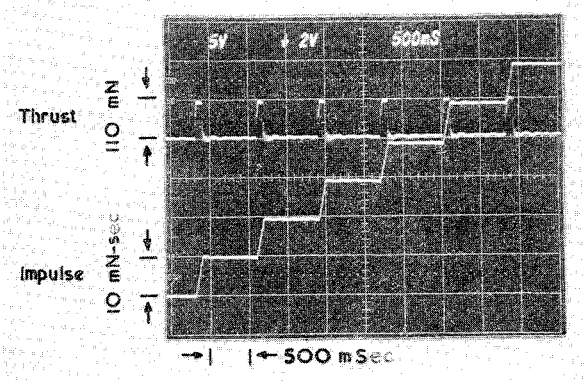

Fig. 16 Impulse produced by consecutive thrust pulses.

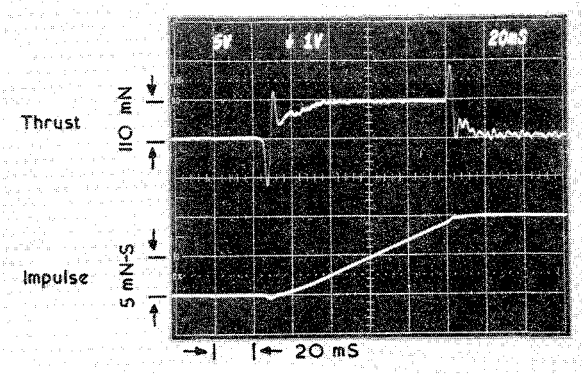

Fig. 17 Impulse produced by single thrust pulse.

are unaffected by the valve reaction transients since these are internal forces.

References

[1] Stott, D., "The Design and Application of Hybrid Hydrazine Resistojets." Paper 9.3, April 1973, *Conference on Electric Propulsion of Space Vehicles,* Culham, England.

[2] Murch, C. K. and Hunter, C. R., "Electrothermal Hydrazine Thruster Development," AIAA Paper 72-451, Bethesda, Md., 1972.

[3] Barber, B. C., "A Fast Response Thrust Transducer for Gas-dynamic Thrusters," RAE TR Royal Aircraft Establishment, Farnborough, England, (in preparation).

[4] Boyd, A. H., "High Response Pulse Rocket Engine Thrust Measurement System," *Instrumentation in the Aerospace Industry,* Vol. 15, 1969, pp. 18–33; also *Proceedings of the 15th International ISA Instrumentation Symposium,*

[5] Crosswy, F. L. and Kalb, H. T., "Investigation of Dynamic Rocket Thrust Measurement Techniques," AEDC-TR-67-202, November 1967, Arnold Engineering Development Center, Tullahoma, Tenn.

[6] Crosswy, F. L. and Kalb, H. T., "Dynamic Compensation and Force Calibration Techniques for a Static and Dynamic Thrust Measurement System," AEDC-TR-68-202, Nov. 1968. Arnold Engineering Development Center, Tullahoma, Tenn.

[7] Crosswy, F. L. and Kalb, H. T., "Performance of a Dynamically Compensated Load Cell Force Measurement System," AEDC-TR-68-211, Nov. 1968, Arnold Engineering Development Center, Tullahoma, Tenn.

[8] Geffe, P. R., *Simplified Modern Filter Design,* London Iliffe Books Ltd., London, England, 1964, p. 67.

[9] Storey, D. J. and Cullyer, W. J., "Active Low-Pass Linear Phase Filters for Pulse Transmission," *Proceedings of the IEE* (Great Britain), Vol. 112, No. 4, April 1965, pp. 661–668.

[10] Gooding, F. E. J. and Good, E. F., "Active Filters—9," *Wireless World,* Vol. 76, No. 1414, April 1970, pp. 188.

AUGUST 1974 J. SPACECRAFT VOL. 11, NO. 8

Electrolytic Capacitor Power Source Design for Quasi-Steady Magnetoplasmadynamic Arcs

MARCO S. DI CAPUA* AND HELMUT L. KURTZ†
Institut für Raumfahrtantriebe, University of Stuttgart, Stuttgart, F.R. Germany

An "*LC*-Ladder" network is investigated theoretically and experimentally to determine the effect of the capacitor series resistance R_C and the inductor series resistance R_L on the shape of the current pulse, on the efficiency of energy transfer, and on the weight of the thruster system. R_C increases the risetime, decreases the duration of the constant current phase, and extends the pulse tail. The deterioration of the pulse is caused by energy dissipation within the network. A small ratio of R_C to the impedance of the network Z_o minimizes this loss. R_L causes a decay of the constant current phase and significant energy losses within the network. The number of elements in the network, multiplied by the ratio R_L to Z_o, must be small to minimize this loss. These losses imply an increased primary power source mass. However, there is a tradeoff between inductor mass (to minimize R_L) and primary power source mass.

I. Introduction

CURRENT interest in electrolytic capacitors as energy storage units for quasi-steady magnetoplasmadynamic (MPD) arcs stems from their desirable electrical characteristics which complement very closely the properties of such accelerators. The capacitor characteristics consist of their ability to store electrical charge at high capacity ($\sim 10^{-3}$ F) and low voltage (<500 v) which enables a power source composed of such units to deliver the long duration (>1 msec), high current pulses ($\sim 10^4$–10^5 amp) which are essential to the proper operation of a self-field quasi-steady MPD accelerator. In addition, electrolytic capacitors have a specific mass (~6 g/joule) which is much smaller than the mass of metallized paper (~14–35 g/joule), impregnated paper (~150 g/joule), or polycarbonate (Mylar, ~150–300 g/joule) capacitors,[1] which provides for added advantage for space applications.

Presented as Paper 73-1107 at the AIAA 10th Electric Propulsion Conference, Lake Tahoe, Nev., October 31–November 2, 1973; submitted October 30, 1973; revision received March 22, 1974. This work was sponsored by the State of Baden-Württemberg, German Federal Republic. The authors gratefully acknowledge the helpful assistance of M. Amin, M. A. Healy, E. Mangold, and H. Opperman during the course of this research.

Index categories: Electric and Advanced Space Propulsion; Plasma Dynamics and MHD; Spacecraft Electric Power Systems.

* Research Associate, currently with Physics International Company, San Leandro, Calif.

† Research Associate.

II. Electrolytic Capacitors

An electrolytic capacitor[2] consists of a metal (Al or Ta) anode plate which is coated by a thin (~1 μm) electrochemically deposited layer of oxide (Al or Ta) dielectric ($\varepsilon = 8$) which forms a semiconductor junction. The other "plate" is an electrolyte retained by a layer of porous paper. A second plate (Al or Ta) establishes contact with the electrolyte. This construction endows the capacitor with some unique properties which are summarized as follows.

a) An extremely large capacitance per unit area, due to the small thickness and large dielectric constant ε of the dielectric, which is further increased (~15 ×) by etching the anode foil. This translates directly into a large capacitance per unit weight.

b) The dielectric-metal semi-conductor junction conducts when the oxide layer is positive with respect to the coated plate. Therefore, the capacitor conducts under a voltage reversal, the uncoated plate oxidizes with a consequent loss of capacitance and gas is formed which eventually destroys the unit. The diode